Hindered and Enhanced Coalescence of Drops in Stokes Flows

M. B. Nemer,[1] X. Chen,[1] D. H. Papadopoulos,[1] J. Bławzdziewicz,[2] and M. Loewenberg[1]

[1]*Department of Chemical Engineering, Yale University, New Haven, Connecticut, USA*
[2]*Department of Mechanical Engineering, Yale University, New Haven, Connecticut, USA*
(Received 10 September 2002; published 17 March 2004)

We analyze axisymmetric near-contact motion of two drops under the action of an external force or imposed flow. It is shown that hydrodynamic stresses in the near-contact region that are associated with the outer (drop-scale) flow can qualitatively affect the drainage of the thin fluid film separating the drops. If this far-field stress acts radially inward, film drainage is arrested at long times; exponential film drainage occurs if this stress acts outward. An asymptotic analysis of the stationary long-time film profile is presented for small-deformation conditions, and the critical strength of van der Waals attraction for film rupture is calculated. The effect of an insoluble surfactant is also considered. Hindered and enhanced drop coalescence are not predicted by the current theories, because the influence of the outer flow on film drainage is ignored.

Because of the relevance of the drop-size distribution for the properties of dispersed fluid-fluid systems, drop coalescence has motivated numerous fundamental investigations [1–7]. Examples of processes where drop coalescence is important include polymer blends [5], and bubble growth in Champagne [8].

Coalescence relies on an agent to push drops together (e.g., body force, external flow), as well as short-range molecular forces (e.g., van der Waals attraction) that rupture the thin liquid film that separates drop interfaces prior to confluence. In many systems, the rate-limiting step for drop coalescence is associated with squeezing fluid out of the flattened thin-film region. Thus, the film-drainage process has been the focus of many studies [1,2,9–11].

For drops that are pressed together in a quiescent fluid, the thin-film-drainage dynamics is reasonably well understood. However, the influence of an ambient flow on the behavior of the near-contact region is a subject of a controversy, which is addressed in our Letter.

According to the current understanding, the direct effect of an ambient flow on the dynamics of the thin-film region is unimportant under small-deformation conditions—the ambient flow field affects drop coalescence only through the hydrodynamic pushing force that it provides [9–13]. Here we show that for drops with tangentially mobile interfaces, this assumption is incorrect: an ambient flow may qualitatively affect film-drainage dynamics. In some cases it prevents drop coalescence and in others results in rapid exponential drainage of the film.

The film thickness h is much smaller than the radius of the flattened near-contact region, thus the lubrication approximation is appropriate. Accordingly, tangential stresses $\mathbf{f}$ on two film interfaces are balanced by the lateral pressure gradient in the film,

$$h\boldsymbol{\nabla}_s p = 2\mathbf{f}. \qquad (1)$$

In the absence of interfacial-tension gradients, $\mathbf{f}$ is equal to the hydrodynamic stress associated with the flow field $\mathbf{v}$ inside of the drops. Under small-deformation conditions, the flow field $\mathbf{v}$ can be linearly decomposed $\mathbf{v} = \mathbf{v}_t + \mathbf{v}_d$ into the local and the far-field (drop-scale) contributions. The local contribution $\mathbf{v}_t$ is driven by the tangential motion of the thin film and vanishes far from the near-contact region; conversely $\mathbf{v}_d$ is driven by the ambient flow and vanishes at the film interfaces. The stress $\mathbf{f}$ has a corresponding decomposition

$$\mathbf{f} = \mathbf{f}_t + \mathbf{f}_d. \qquad (2)$$

Under small-deformation conditions, the drop-scale flow and corresponding stress correspond to a local stagnation-point flow.

The local stress component $\mathbf{f}_t$ was included in previous analyses in the form of a boundary-integral term [14]; however, the far-field stress $\mathbf{f}_d$ was ignored. To show that the far-field stress component can substantially affect film-drainage dynamics, we first note that the $\mathbf{f}_d$ is insensitive to the film profile, because it varies on the drop scale and is nonzero on the film interface. Given that $\boldsymbol{\nabla}_s p$ is also insensitive to film thickness, we find that $\mathbf{f}_d \approx h\boldsymbol{\nabla}_s p$ for sufficiently thin films (e.g., at long times). Hence, $\mathbf{f}_d$ must be retained in the lubrication stress balance (1), contrary to the current theories.

The boundary-integral simulations and asymptotic analysis presented below show that the far-field stress component $\mathbf{f}_d$ can arrest or accelerate the drainage of the film. The results thus demonstrate the significance of the stress associated with the drop-scale flow, consistent with argument above. We consider these effects for axisymmetric near-contact motion of two drops $i = 1, 2$ subjected to body forces or an imposed linear flow

$$\mathbf{F}_i^e = F_i^e \hat{\mathbf{e}}_z, \qquad \mathbf{u}^e = G\left(\frac{1}{2}r\hat{\mathbf{e}}_r - z\hat{\mathbf{e}}_z\right). \qquad (3)$$

Here (r, z) are cylindrical coordinates with unit vectors $\hat{\mathbf{e}}_r$, $\hat{\mathbf{e}}_z$ and origin at the center of the gap between the drops; drop (1) is in the half-space $z < 0$. The suspending fluid has viscosity μ, the drops have viscosity $\lambda\mu$, and except as noted, the interfacial-tension σ_0 is constant and molecular interactions are absent. The undeformed-drop radii are a_1, $a_2 = ka_1$. Stokes flow conditions are assumed thus, the velocity field depends linearly on G and F_i^e.

Henceforth lengths are rescaled by $a = (a_1^{-1} + a_2^{-1})^{-1}$, stresses by σ_0/a, force by $\sigma_0 a$, velocity by σ_0/μ, and time by $\mu a/\sigma_0$. In the dimensionless formulation, the system dynamics are characterized by the force and flow-strength parameters

$$\hat{F}_i^e = \frac{F_i^e}{\sigma_0 a}, \qquad \hat{G} = \frac{\mu Ga}{\sigma_0}. \qquad (4)$$

Surfactants and van der Waals attraction introduce additional parameters which are briefly considered herein.

Boundary-integral simulations.—Figures 1 and 2 depict the film evolution for parameter values corresponding, respectively, to a far-field stress directed inward and outward. In the first case, a stationary film profile is attained at long times; in the second case, the film drains exponentially. For $f_d = 0$, the film thickness decays algebraically at long times [15,16]. The current theories neglect the far-field stress component and thus predict algebraic film drainage for all parameter values, which is at odds with the numerical results shown in Figs. 1 and 2.
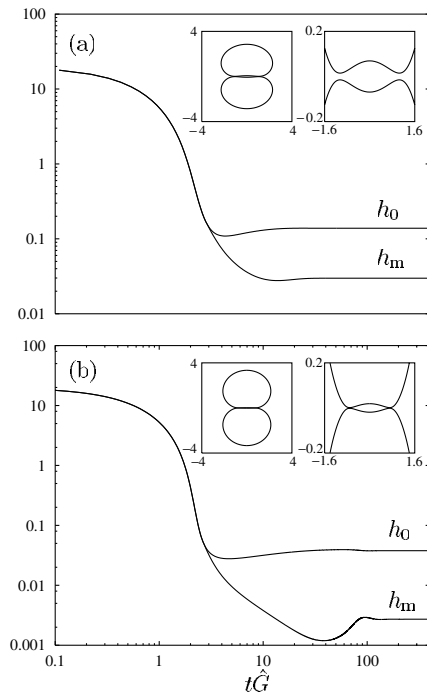

FIG. 1. Evolution of center h_0 and minimum h_m film thickness for equal-size drops with $\lambda = 1$ in straining flow; $\hat{F}_1^e = \hat{F}_2^e = 0$ and (a) $\hat{G} = 0.05$, (b) $\hat{G} = 0.02$. Insets show stationary drop shape and film profile.

Asymptotic analysis.—In the weak-forcing regime, the extent of the thin-film region r_∞ is small, and the drops remain nearly spherical. Moreover, the relative drop velocity is small because of large lubrication resistance in the flattened near-contact region. Thus, the asymptotic form of the hydrodynamic forces $F_i^H(k, \lambda)$ on the drops and the far-field stresses f_d, generated by the flow far from the near-contact region, correspond to the forces and stresses on spherical drops in point contact, with no relative motion.

Accordingly, the hydrodynamic forces are given by a linear resistance relation [17], and the far-field stress component $\mathbf{f}_d = f_d\hat{\mathbf{e}}_r$ is given by the expressions

$$f_d = -rS, \qquad r\lambda \ll 1, \qquad (5)$$

and

$$\lambda^{-1}S = \frac{(k - 1)k}{4(1 + k)^3}\hat{U} + \frac{4k - 1 - k^2}{2(1 + k)^2}\hat{G}, \qquad (6)$$

which were obtained by solving Stokes equations in tangent-sphere coordinates. Here, $\hat{G}$ is the dimensionless strain-rate (4) and $\hat{U}$ is the pair migration velocity of the drops. For unequal-size drops $f_d = \frac{1}{2}[f_d^{(1)} + f_d^{(2)}]$ is the mean of the far-field stresses on both interfaces.

According to the above relations, the far-field stress can be directed inward or outward. In particular, for drops in axisymmetric compressional flow ($\hat{G} > 0$) with no net force, the far-field stress is directed inward for $k_{crit}(\lambda) < k < k_{crit}^{-1}(\lambda)$, and outward for k outside of this range. Equation (6), supplemented by the hydrodynamic forces that determine $\hat{U}$, yields $k_{crit}(\lambda) = 0.351 \pm 0.005$ for $0 < \lambda < \infty$.

The effect of the external flow on the film dynamics is transmitted through the far-field stress f_d, rather than the velocity field on the film interface v_t which only determines f_t. Unlike f_t, the stress f_d is insensitive to the film profile, because it varies on the outer length scale a. This
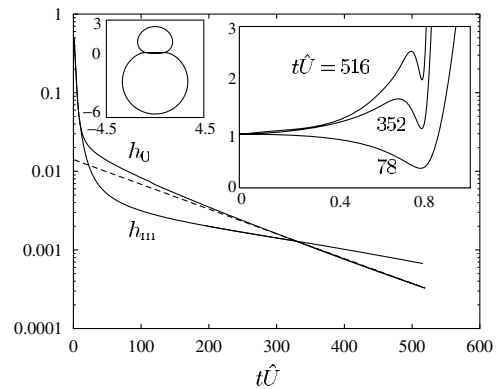

FIG. 2. Evolution of center h_0 and local-minimum h_m film thickness for unequal-size drops with $a_2/a_1 = \frac{1}{2}$ and $\lambda = 1$ in buoyancy motion; $\hat{F}_1^e = 8\hat{F}_2^e = 4\pi$, $\hat{G} = 0$. Exponential fit (dashed line). Insets show long-time drop shape and film profile h/h_0 at indicated times.

conclusion is supported by the results of our numerical simulations, which indicate that the relative accuracy of the asymptotic expressions (5) and (6) is $O(r_\infty)$.

The far-field stress f_d may be incorporated into the lubrication description of the near-contact region. Here we focus on the stationary profile $h(r)$ corresponding to an inward-directed far-field stress. At stationary state, the tangential stress balance (1) gives the scaling $v_t \sim fh$ for the interfacial velocity. The local stress component scales as $f_t \sim v_t/l$, where $l \gg h$ is the lateral length scale of the film. Accordingly, $f_t \sim (h/l)f$, which implies that f_t can be neglected in the stress balance (1). For axisymmetric configurations, this approximation and Eq. (5) yields

$$hp' = -2rS, \qquad (7)$$

where prime denotes the derivative with respect to r. The tangential stress balance (7) and normal balance

$$p = 1 - \frac{1}{2} r^{-1}(rh')', \qquad (8)$$

supplemented with boundary conditions

$$h'(0) = 0, \qquad \lim_{r \to \infty} p(r) = 0, \qquad (9)$$

and the force balance

$$F_c = 2\pi \int_0^\infty pr\,dr, \qquad (10)$$

yield a closed set of equations for the stationary film profile. Here $F_c = \frac{1}{2}(\hat{F}_-^{e} + F_-^{H})$, where $F_- = F_1 - F_2$, is the total pushing force, which is balanced by the contact force associated with pressure in the deformed near-contact region.

As illustrated by the insets in Fig. 1, the fluid film between the drops has a dimpled shape with maximum thickness $h_0 = h(0)$ at the axis of symmetry and minimum h_m at $r_m \approx r_\infty$, where

$$r_\infty = (F_c/\pi)^{1/2} \qquad (11)$$

is the extent of the thin-film region according to Eqs. (8) and (10). In the weak-forcing regime, where $h_0 \gg h_m$, the asymptotic film profile can be obtained by matching asymptotic solutions for the central "dome" region $r < r_\infty$ and "rim" region $r \approx r_m$. The matching procedure yields

$$h(r) = \begin{cases} h_0\bar{h}(\bar{r}) + h_m[\tilde{h}(\tilde{x}) - (\frac{8}{3}Q_*)^{1/2}(-\tilde{x})^{3/2}], & \bar{r} \lesssim 1, \\ h_m[h(\tilde{x}) - \tilde{x}^2] - \log\bar{r} + \frac{1}{2}\bar{r}^2 - \frac{1}{2}, & 1 < \bar{r} \ll a/r_\infty, \end{cases} \qquad (12)$$

where $\bar{r} = r/r_\infty$ and $\tilde{x} = (r - r_m)/h_m^{1/2}$ are the dome- and rim-scale variables, respectively. The shape functions $\bar{h}$ and $\tilde{h}$ satisfy the asymptotic dome and rim equations

$$\bar{h}[\bar{r}^{-1}(\bar{r}\bar{h}')']' = B_*\bar{r}, \qquad (13a)$$

$$\tilde{h}'''\tilde{h} = Q_*, \qquad (13b)$$

where prime denotes differentiation with respect to the corresponding variable $\bar{r}$ or $\tilde{x}$. The shape functions satisfy the rescaled boundary conditions (9) and (10), and the matching conditions $\bar{h}(1 - \bar{s}) = O(\bar{s}^{3/2})$ for $\bar{s} \ll 1$ and $\tilde{h}(-\tilde{s}) = O(\tilde{s}^{3/2})$ for $\tilde{s} \gg 1$ which require

$$B_* = 6.39, \qquad Q_* = 0.439. \qquad (14)$$

The shape functions $\bar{h}$ and $\tilde{h}$ are plotted in Fig. 3.

From the rescaled variables in Eq. (12), we obtain

$$h_0 = 2\pi^{-1}B_*^{-1/2}F_c S^{1/2}, \qquad (15)$$

$$h_m = 16\pi^{-1}Q_*^{-2}S^2 F_c. \qquad (16)$$

For drops in straining flow, these expressions yield $h_0 \sim \hat{G}^{3/2}$ and $h_m \sim \hat{G}^3$. In Fig. 4, this asymptotic behavior is compared with results of boundary-integral simulations. The asymptotic theory is accurate to $O(r_\infty)$, consistent with the accuracy of the approximation for the tangential stress (5) and (6).

For sufficiently thin films, van der Waals attraction is important and can lead to film rupture in the rim. The effect of van der Waals stresses $A(6\pi h^3)^{-1}$ is included by modifying the stationary rim Eq. (13b),

$$\tilde{h}\tilde{h}''' = Q_* - \tilde{A}\tilde{h}'\tilde{h}^{-3}, \qquad (17)$$

where $\tilde{A} = \pi A h_m^{-3}$. Here A is the Hamaker constant normalized by $\sigma_0 a^2$, and h_ms the minimal film thickness (16) in the absence of van der Waals attraction. The minimum thickness h_m^A in the presence of van der Waals attraction is obtained by numerical integration of Eq. (17) with appropriate boundary conditions. The results shown in Fig. 5 reveal a stable and an unstable branch of solutions for $\tilde{A} < \tilde{A}_{\mathrm{crit}}$, and a turning point at

$$\tilde{A}_{\mathrm{crit}} = 1.49. \qquad (18)$$

The presence of a nondiffusing insoluble surfactant on the drop interfaces leads, at steady state, to the formation of tangentially-immobile surfactant caps. If $f_d^{(i)} < 0$, a cap forms at the center of the thin-film region on drop
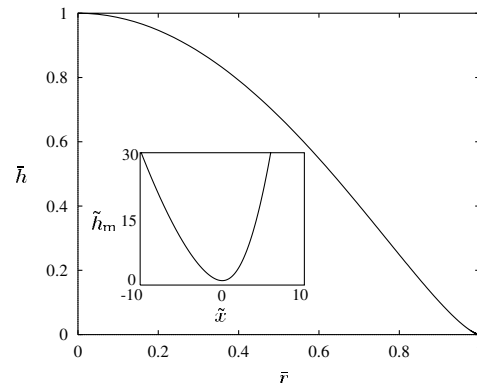

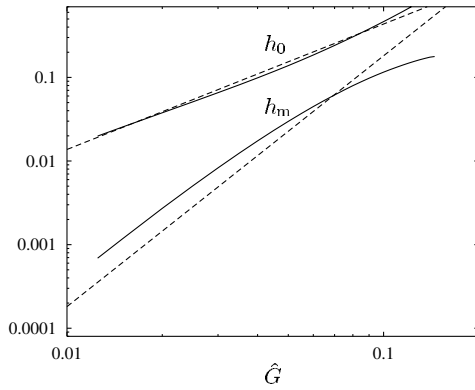FIG. 3. Asymptotic solutions of dome and rim (inset) profiles.

FIG. 4.   Stationary center h_0 and minimum h_m film thickness for equal-size drops with $\lambda = 1$ in straining flow versus flow-strength parameter; $\hat{F}_1^e = \hat{F}_2^e = 0$. Numerical simulations (solid lines); asymptotic formulas (15) and (16) (dashed lines).

FIG. 5.   Minimal gap versus Hamaker parameter. Stable branch (solid line); unstable branch (dashed line).

i, and the stress balance on the cap is $d\sigma^{(i)}/dr = -f_d^{(i)}$, where $\sigma^{(i)}$ is the interfacial-tension distribution.

By integrating this stress balance and using the surfactant equation of state, the cap radii $r_c^{(i)}$ can be related to the amount of surfactant on the drop interfaces. For $r_c^{(i)} > r_\infty$, the flow in the thin film is shielded from the far-field stress $f_d^{(i)}$ by the stagnant cap. For $r_c^{(i)} < r_\infty$, the rim Eq. (13b), and thus the film profile in the rim region, are unaffected by the surfactant. The critical molar quantity of surfactant $n^{(i)}$ on the interface of drop i, corresponding to $r_c^{(i)} = r_\infty$, is given by

$$4\pi n^{(i)} RT/\sigma_0 a^2 = S^{(i)} F_c^2, \tag{19}$$

where R is the gas constant, T is temperature, and $S^{(i)}$ is the stress coefficient defined by Eq. (5) with f_d replaced by $f_d^{(i)}$.

Thus far, we have assumed an inward-directed far-field stress f_d. For an outward-directed far-field stress [$S < 0$ in Eq. (6)], film drainage is enhanced. For sufficiently thin films, $p'h \ll f_d, f_t$. Accordingly, the appropriate tangential stress balance, derived from Eqs. (1) and (2), is $f_d = -f_t$. Given the scalings $f_t \sim v_t/r_\infty$ and $f_d \sim r_\infty S$, and using mass conservation in the film $dh/dt \sim v_t h/r_\infty$, we find that the film drains exponentially at long times

$$dh/dt \sim Sr_\infty h. \tag{20}$$

Figure 2 shows that the above scaling applies in the central region of the film.

In this Letter we focused on axisymmetric collisions of drops. We have shown that the tangential stress associated with flow far from the near-contact region hinders film drainage when it acts radially inward, and enhances drainage when it acts radially outward. The effect of the drop-scale flow on off-axis collisions requires further study. However, our scaling analysis of Eq. (1) indicates that for sufficiently small gaps the stress $\mathbf{f}_d$ cannot be neglected also in nonaxisymmetric configurations.
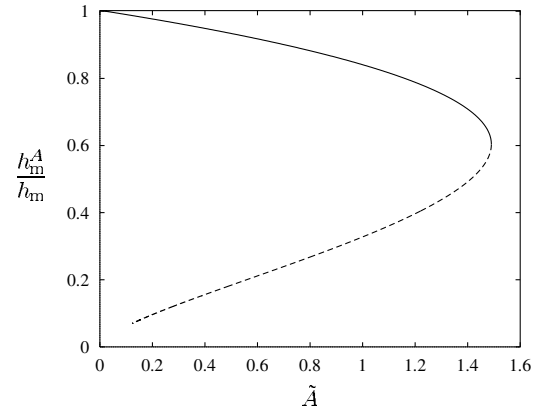
Approximations which ignore the effect of the drop-scale flow on the thin-film dynamics need to be reexamined.

[1] K. Hool, R. Saunders, and H. Ploehn, Rev. Sci. Instrum. **69**, 3232 (1998).
[2] T. Chuang and R. Flumerfelt, Rev. Sci. Instrum. **68**, 3839 (1997).
[3] A. Nandi, A. Mehra, and D. Khakhar, Phys. Rev. Lett. **83**, 2461 (1999).
[4] Y. Amarouchene, G. Cristobal, and H. Kellay, Phys. Rev. Lett. **87**, 206104 (2001).
[5] I. Fortelny and A. Zivny, Polymer **39**, 2669 (1998).
[6] D. Li and S. Liu, Langmuir **12**, 5216 (1996).
[7] G. Neitzel and P. Dell'Aversana, Annu. Rev. Fluid Mech. **34**, 267 (2002).
[8] J. Senee, B. Robillard, and M. Vignes-Adler, Food Hydrocolloids **13**, 15 (1999).
[9] S. G. Yiantsios and R. H. Davis, J. Colloid Interface Sci. **144**, 412 (1991).
[10] A. Saboni, C. Gourdon, and A. K. Chesters, J. Colloid Interface Sci. **175**, 27 (1995).
[11] M. A. Rother, A. Z. Zinchenko, and R. H. Davis, J. Fluid Mech. **346**, 117 (1997).
[12] M. A. Rother and R. H. Davis, J. Colloid Interface Sci. **214**, 297 (1999).
[13] M. A. Rother and R. H. Davis, Phys. Fluids **13**, 1178 (2001).
[14] K. M. Jansons and J. R. Lister, Phys. Fluids **31**, 1321 (1988).
[15] A. F. Jones and S. D. R. Wilson, J. Fluid Mech. **87**, 263 (1978).
[16] M. B. Nemer, X. Chen, J. Błyawzdziewicz, and M. Loewenberg, Bull. Am. Phys. Soc. **46**, 140 (2001).
[17] L. D. Reed and F. A. Morrison, Int. J. Multiphase Flow **1**, 573 (1974).